Effect of Tungsten (W) on Creep Properties of 9Cr-3W-3Co-Nd-B Steel Weld Metals

Hiromi OYAMADA*1 · Hideaki TAKAUCHI*1 · Shigenobu NANBA*2

*1 Welding Process Department, Technical Center, Welding Business
*2 Materials Research Laboratory, Technical Development Group

Abstract

ASME Gr. 93 steel is a heat-resistant steel, in which creep strength is increased by adding elements such as W and B to the conventional 9% Cr ferritic heat-resistant steel. An investigation has been conducted on the effects of W addition on the creep rupture time and metallographic structure of weld metals for Gr.93 steel. The results of the creep rupture test on weld metals with varying additions of W show that creep rupture time increases with the increasing amount of W. Observations of specimens thermally aged at 650℃ have confirmed the presence of the Laves phase, suggesting that the increase in creep rupture time is attributable to particle dispersion strengthening by the Laves phase. Increasing the additive amount of W increases the number density of the Laves phase and, furthermore, suppresses the coarsening of the Laves phase during thermal aging. The coarsening rate of the Laves phase during thermal aging has been in good agreement with the calculated value obtained from the theoretical equation for Ostwald ripening. Like $M_{23}C_6$, the Laves phase may contribute to the creep strengthening by suppressing the coarsening of the lath size.

Introduction

In Japan, the 6th Strategic Energy Plan [1] was approved by the Cabinet in October 2021. As a result of this policy, it is considered that the proportion of electricity generated by coal-fired thermal power will decrease, and the predominant focus in thermal power generation will shift towards co-combustion and dedicated combustion of non-carbon fuels such as ammonia and hydrogen. Since thermal power generation is assumed to function as a regulating power source to supplement the unstable renewable energy supply, the frequency of the startup and shutdown cycle is expected to increase compared with conventional operations, and the thermal fatigue property of boilers is a concern. One of the methods to improve thermal fatigue properties is to enhance the strength of steel and thin out piping. The benefits associated with the increased strength of steel include the reduction of maintenance costs by extending the lifespan of piping.

ASME Grade 93 steel (9Cr-3W-3Co-Nd-B steel) has improved the creep strength and creep rupture ductility of conventional 9Cr ferritic heat-resistant steel [2]. Characteristics of this steel grade include the addition of boron to suppress formation of fine-grains in the heat affected zone (HAZ) of welding and improved creep strength. Additionally, tungsten (W) is added to achieve solid-solution strengthening and particle dispersion strengthening with the Laves phase (Fe_2W) [2]. The addition of boron is reported by Nako et al. [3] to contribute to the creep strengthening of weld metal for ASME Grade 92 (9Cr-1.8W-0.5Mo-Nb-V) steel by suppressing the coarsening rate of $M_{23}C_6$. Fedoseeva et al. have reported that increasing the W content from 2 mass% to 3 mass% in ASME Grade 92 steel improves its creep strength up to 10,000 hours, but the effect of W on creep strength disappears at 100,000 hours [4]. However, it is not clear whether the weld metal of Grade 93 steel exhibits a similar trend. This paper focuses on W and reports the results of investigation into the way in which W addition to Grade 93 steel weld metal affects the creep rupture time and metallographic structure.

1. Experimental method

1.1 Test Material

Weld metals were produced using a covered electrode having a core diameter of ϕ4.0 mm. For two types of weld metal with different compositions (A and B), specimens were prepared by varying the W content within the range of 1.6 to 2.8 mass% for each composition. The welding conditions were described as follows, polarity: direct current electrode positive (DCEP), heat input: 1.5 to 2.5 kJ/mm. The produced weld metals were subjected to post-weld heat treatment (PWHT) at 760℃ for 4 hours. The chemical compositions of the weld metals are shown in **Table 1**.

1.2 Creep rupture test

The all-weld-metal creep specimens were taken from the center of weld metals in the longitudinal direction. The round bar specimens have a nominal diameter of ϕ6 mm, and the nominal gauge length of 30 mm. The test temperature was set at 650℃, with stress conditions of 170 MPa and 80 MPa.

Table 1 Chemical compositions in weld metals

(mass%)

Specimen mark	W	C	Si	Mn	Ni	Cr	V	Co	B	Nb	N
2.8W-A	**2.8**	0.1	0.3 ~0.4	0.5	0.5	9	0.2	3	0.007 ~0.012	0.05 ~0.06	0.02
1.6W-A	**1.6**										
2.7W-B	**2.7**	0.1	0.3	0.5	0.5	9	0.2	3	0.004	0.08	-
1.7W-B	**1.7**										

1.3 Metallographic observation

The field emission scanning electron microscope (hereinafter referred to as "FE-SEM") was used to evaluate the microstructure morphology of the weld metal. The observation positions were set to correspond to the reheated zone along the axis of the creep specimens of the weld metal. Elemental mapping data was obtained using Energy Dispersive X-ray spectroscopy (hereinafter referred to as "EDX") to identify the precipitates.

2. Experimental results and discussion

2.1 Effect of W on creep rupture time

Fig. 1 shows the relationship between the creep rupture time and the W content in the weld metal under various stress conditions. Regardless of the stress conditions, increasing W tended to improve the creep rupture time. According to Kimura et al.[5], simultaneous addition of W and Co in 15Cr ferritic heat-resistant steel enhances creep strength, and the contributing factor may be precipitates. Morimoto et al.[6] state that when the W content in the weld metal is between 1.6 to 1.7 mass%, the Laves phase precipitates during creep rupture testing at 600℃ (after approximately 100 to 1,000 hours). In this study, microstructure observations were conducted considering the possibility that the Laves phase may have an impact on creep rupture time.

2.2 Effect of W on microstructure of weld metals

The microstructures of the weld metal were observed after PWHT and subsequent thermal aging at 650℃ for 3,000 to 20,000 hours. It should be noted that, due to the absence of applied stress, the thermal aging causes diffusion to progress less readily compared with the creep rupture test. However, considering the cost of the tests, it was adopted for the purpose of understanding the trends. **Fig. 2** shows the backscattered electron image taken by FE-SEM, and **Fig. 3** shows the EDX elemental mapping images of 2.8W-A after 5,000 hours of

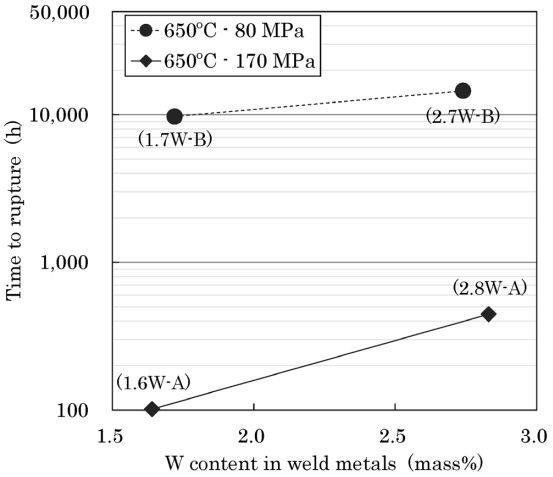

Fig.1 Relationship between time to rupture and W content in weld metals

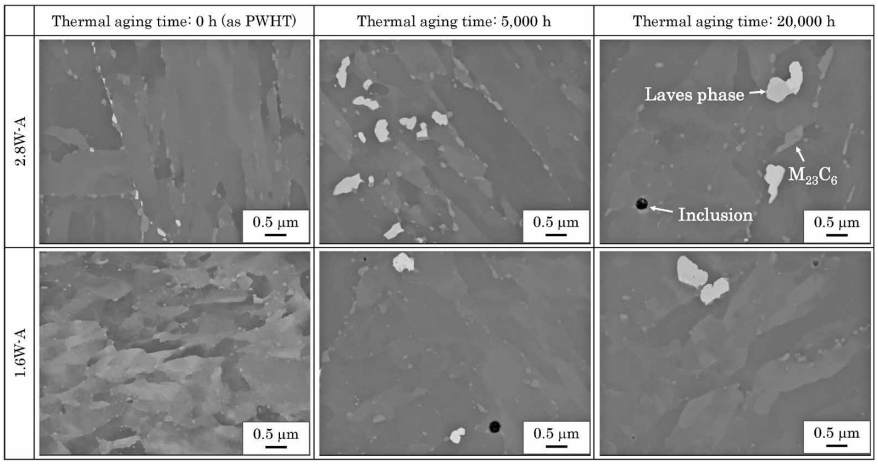

Fig.2 Backscattered electron images of weld metals

thermal aging. In FE-SEM observation, two types of precipitates, white and gray in color, were observed. The precipitation mainly occurred at the locations identified as lath boundaries within the martensite structure.

No white precipitates were observed after PWHT of 1.6W-A, but they were confirmed after 5,000 hours of thermal aging. However, the number density of these precipitates is significantly lower compared with 2.8W-A. The white precipitates observed in 2.8W-A were nearly elliptical after PWHT, and they grew with increasing thermal aging time. On the other hand, the grain size of the gray precipitates was smaller than that of the white precipitates and the shape is closer to a circle or ellipse. From the EDX elemental mapping, it has been confirmed that W is concentrated in the white precipitates, while Cr is concentrated in the gray precipitates.

The precipitates formed in equilibrium at 760℃ and 650℃ based on the composition shown in Table 1 were calculated by means of the thermodynamic calculation software, Thermo-Calc (Database: TCFE9). The results are presented in **Table 2**. The calculated phases include $M_{23}C_6$, the Laves phase, MX, Cr_2B, and Z phase. The particle diameter of MX in 9Cr ferritic weld metal is reported to be on the order of several tens of nanometers[7], the amount of Cr_2B is low in equilibrium, and Z phase is said to be formed during long-term thermal aging exceeding several tens of thousands of hours. Based on these factors, most of the precipitates seen in Fig. 2 are $M_{23}C_6$ and the Laves phase. According to these results, it is concluded that the white precipitates are the Laves phase, while the gray precipitates are Cr-dominant $M_{23}C_6$. Subsequent discussions focus on evaluating the Laves phase, where the effect of W is more prominently observed. The black inclusions present in some specimens are oxide compounds generated during the shielded metal arc welding.

Fig. 4 shows the average equivalent circle radius and number density of the Laves phase with thermal aging time, obtained from Fig. 2. In the case of 1.6W-A, no Laves phase has been observed after PWHT, which is consistent with the results from Thermo-Calc calculations. The equivalent circle radius of the Laves phase tends to increase with the progression of thermal aging for both 2.8W-A and 1.6W-A. However, in the case of 2.8W-A, the coarsening stagnates at around 150 nm after thermal aging for more than 10,000 hours. In contrast, the coarsening of 1.6W-A progresses to approximately 200 nm after thermal aging for 20,000 hours. The number density of the Laves phase increases during relatively short-term thermal aging after PWHT and then decreases until 20,000 hours of thermal aging. At any thermal aging time, the number density of the Laves phase of 2.8W-A is greater than that of 1.6W-A.

The formula for the creep strain rate $\dot{\varepsilon}$ of particle dispersion strengthening materials is known to be as follows[8]:

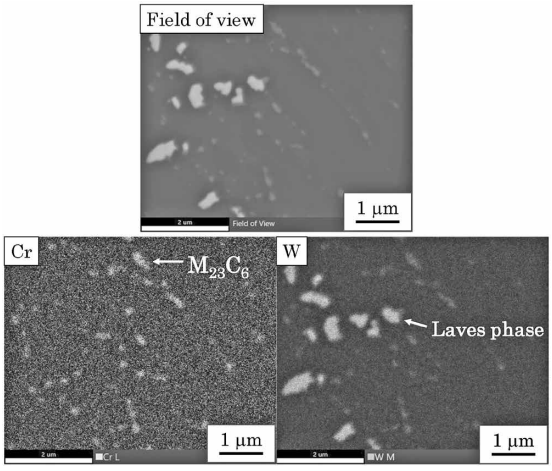

Fig.3 EDX mapping images of 2.8W-A after thermal aging for 5,000 h

Table 2 Volume fraction of precipitates at PWHT temp. and thermal aging temp. calculated by Thermo-Calc with TCFE9 database

(vol.%)

Specimen mark	Calculated temp.	$M_{23}C_6$	**Laves phase**	MX	Cr_2B	Z phase
2.8W-A	760°C *[PWHT]*	1.49	**0.60**	0.03	0.10	0.21
	650°C *[Aging]*	1.55	**1.86**	0.00	0.10	0.25
1.6W-A	760°C *[PWHT]*	1.31	**0.00**	0.19	0.18	0.00
	650°C *[Aging]*	1.42	**0.65**	0.03	0.18	0.24

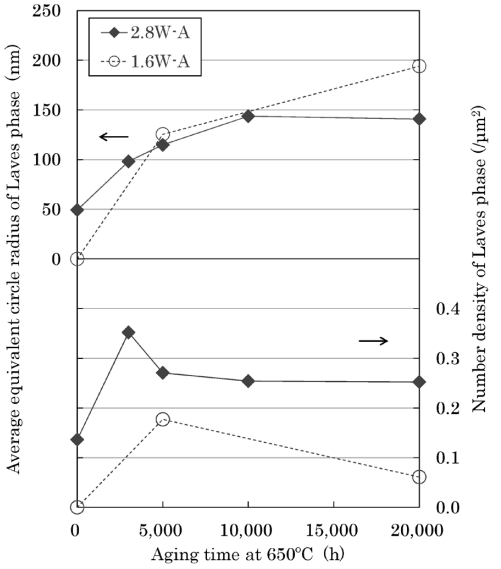

Fig.4 Change in average equivalent circle radius and number density of Laves phase with thermal aging

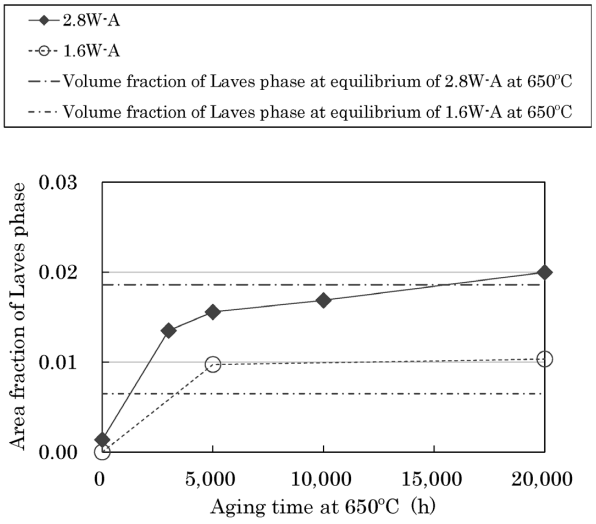

Fig.5 Change in amount of Laves phase with thermal aging

$$\dot{\varepsilon} = \dot{\varepsilon}_0 \left(\frac{\sigma - \sigma_{th}}{E} \right)^m \frac{D}{b^2} \quad \cdots\cdots (1)$$

wherein, D is the diffusion coefficient, E is the Young's modulus, b is the length of the Burgers vector, and the coefficients $\dot{\varepsilon}_0$ and the effective stress exponent m are material constants. σ_{th} is the threshold stress, below which the creep strain rate is assumed to be zero, and is independent of the external stress σ.

The threshold stress σ_{th} is known to be inversely proportional to the interparticle spacing, and the creep strength is improved by decreasing the interparticle spacing. It is inferred that increasing the W content results in a higher number density of the Laves phase and a smaller interparticle spacing, thereby increasing the creep rupture time.

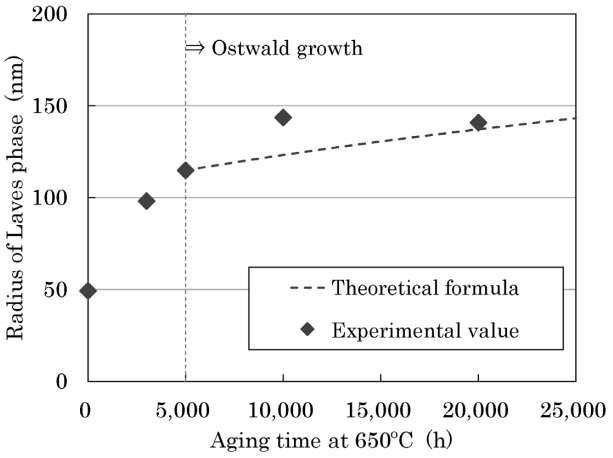

Fig.6 Comparison of theoretical formula and experimental values of Ostwald ripening in the Laves phase

2.3 Thermodynamic considerations

Fig. 5 shows the change in the precipitate amount of the Laves phase with aging time measured through FE-SEM observations. The dashed lines in Fig. 5 represent the volume fraction of the Laves phase in equilibrium at 650℃ of 2.8W-A and 1.6W-A, as indicated in Table 2. For both 2.8W-A and 1.6W-A, the precipitate amount of the Laves phase reaches equilibrium after approximately 5,000 hours or more of thermal aging. Subsequently, the Laves phase became larger and the number density decreased. It is suggested that the Ostwald ripening of the Laves phase is occurring. The theoretical formula for the Ostwald ripening is represented by the following equation:

$$r^3 - r_0^3 = kt \quad \cdots\cdots (2)$$

$$k = \frac{8}{9} \frac{\sigma V^P}{\sum_i^C \frac{(x_i^P - x_i^M)^2}{x_i^M D_i / RT}} \quad \cdots\cdots (3)$$

wherein, r and r_0 are the particle radii of the precipitates at any point during thermal aging and at the beginning of Ostwald ripening, respectively, t is the thermal aging time, σ is the interface energy between the matrix and precipitates, D_i is the diffusion coefficient of solute atom i in the matrix, V^P is the molar volume of precipitates, x_i^P is the concentration of solute atom i in the precipitates, x_i^M is the concentration of solute atom i in the matrix, R is the gas constant, and T is the absolute temperature.

Fig. 6 compares the Ostwald ripening process of the Laves phase derived from the theoretical formula to the experimental values. As mentioned above, the time for the precipitate amount of the Laves phase to reach equilibrium is approximately

5,000 hours. Hence, the theoretical formula has been calculated assuming that Ostwald ripening begins at the point when the thermal aging time reaches 5,000 hours. The theoretical formula shows excellent agreement with the experimental values. The average equivalent circle radius of the Laves phase is approximately 150 nm after thermal aging for 10,000 hours at 650℃, as determined from experimental values. The coarsening rate of the Laves phase during thermal aging does not always coincide with the coarsening rate of the Laves phase during creep rupture test because the creep rupture specimen has been applied stress. However, it is inferred that the particle radius of the Laves phase coarsened to more than about 150 nm under the condition of the creep rupture test time exceeding 10,000 h. Fedoseeva et al. reported that the dislocation pinning force of the Laves phase in 9Cr-3W steel significantly decreases when the creep rupture time exceeded approximately 2,000 hours at 650℃ and 100-220 MPa [4]. However, in this study, it is demonstrated that an increase in W content contributes to the improvement of creep rupture time even when the rupture time is 10,000 to 20,000 hours. This suggests that the Laves phase is effective in increasing the creep rupture time of the weld metal even if it coarsens to a radius of more than 150 nm. As the mechanisms by which precipitates contribute to the creep strengthening of ferritic heat-resistant steel, dislocation pinning, suppression of martensitic lath coarsening, and strengthening of grain boundaries are mentioned. The contribution of the Laves phase to the dislocation pinning may be small, and the MX which exists finely in the grain is more effective for dislocation pinning than the Laves phase which exists in the grain boundary. It is suggested that the coarsening of martensite lath during creep was suppressed by the Laves phase on grain boundaries which may be martensite lath. $M_{23}C_6$ is known to exist along lath boundaries as well as the Laves phase and is effective in inhibiting the coarsening of the martensite microstructure [9], and in the case of 2.8W-A, the addition of W may have enhanced the effect by increasing the precipitates formed on the grain boundary.

Conclusions

The effect of W addition on creep rupture time and microstructure for Gr.93 steel weld metal was investigated. The main results can be summarized as follows:

1. The creep rupture time at 650℃ improved with increasing W content in the weld metal regardless of the stress condition.
2. The average equivalent circle radius of the Laves phase coarsens with the progress of thermal aging at 650℃. After 20,000 hours of aging, the average equivalent circle radius of the Laves phase is around 150 nm for W content of 2.8 mass%, while it grows to approximately 200 nm for W content of 1.6 mass%. The number density of the Laves phase increases throughout the period of 3,000 and 5,000 hours of thermal aging after PWHT, subsequently decreasing.
3. The creep rupture time of 2.8 mass% W is higher than that of 1.6 mass% W, and this is considered to be due to the high number density and narrow particle spacing of the Laves phase.
4. The formation of the Laves phase generally reaches an equilibrium amount after thermal aging for approximately 5,000 hours. Subsequently, coarsening of the Laves phase and the decrease of the number density are considered to cause Ostwald ripening. The experimental values and theoretical formula of Ostwald ripening exhibit good agreement.
5. Even under conditions where the creep rupture time is around 10,000 hours, the addition of W remains effective in increasing the creep rupture time. The Laves phase, is considered to be effective for creep strengthening, even if it coarsens to about 300 nm. Similar to $M_{23}C_6$, the Laves phase may enhance creep rupture time by suppressing the coarsening of lath size.

References

1) Ministry of Economy, Trade and Industry. The 6th Strategic Energy Plan. October 2021 https://www.enecho.meti.go.jp/category/others/basic_plan/, (reference on November 30, 2022).
2) A. Iseda et al. "The Thermal and Nuclear Power Generation Convention Collected Works." Thermal and Nuclear Power Energy Society, 2016, Vol.12, pp.49-55.
3) H. Nako et al. "Preprints of the National Meeting of JWS.", Japan Welding Society, 2017, p.92.
4) A. Fedoseeva et al. "Metals." 2017, Vol.7, Issue 12, Article 573.
5) K. Kimura et al. "ISIJ International." 2001, Vol.41, pp.S121-S125.
6) H. Morimoto et al. "Quarterly Journal of the Japan Welding Society." 1998, Vol.16, No.4, pp.512-521.
7) Y. Banno et al. "Journal of the Japan Welding Society." 2016, Vol.85, No.6, pp.581-587.
8) K. Maruyama et al. "Kouonkyodo no Zairyokagaku (Revised Edition: Materials Science of High-Temperature Strength.) (in Japanese)" Revised 1st edition, Uchida Rokakuho, 2002, p.177.
9) F. Abe. "Bulletin of The Iron and Steel Institute of Japan (Ferrum)." 2012, Vol.17, No.8, pp.560-564.